Housing & Building National Research Center
HBRC Journal

المركز القومي لبحوث الإسكان والبنـاء
المجـلـة العلميـة

10 August , 2014

HBRCJ-D-14-00060

Dear: **Mohamed M. EL-Attar, Hossam Z. El-Karmoty and Amal A. EL-Moneim**

On behalf of the Board of Directors of the HBRC Journal, I'm pleased to inform you that your paper entitled: **"The behavior of ultra-high-strength reinforced concrete columns under axial and cyclic lateral loads"**

Has been accepted for publication in condition that you fulfill all Elsevier comments later on.

Thanks for your interest in our journal and we hope to receive more publications from you in the near future.

Thank you for your contribution to HBRC International Journal.

With my best regards,

Head of the Board of Editors

Dr. Chada Ojaa

Prof. Dr. Adel Ibrahim Elmallawany

Housing & Building National Research Center – 87 Tahrir Street, Dokki-Giza, Egypt PO BOX: 1770 Cairo
www.hbrc-journal.gov.eg
http://www.journals.elsevier.com/hbrc-journal
, email: journal@hbrc.edu.eg , hbrc.journal@gmail.com
Phone: +202-7617062, +202-3351564 Fax: +202-3351564, +202-3367179)

ARTICLE IN PRESS

HBRC Journal (2015) xxx, xxx xxx

Housing and Building National Research Center

HBRC Journal

http://ees.elsevier.com/hbrcj

The behavior of ultra-high-strength reinforced concrete columns under axial and cyclic lateral loads

Mohamed M. EL-Attar [a], Hossam Z. El-Karmoty [b,*], Amal A. EL-Moneim [c]

[a] *Structural Engineering Department, Faculty of Engineering, Cairo University, Cairo, Egypt*
[b] *Housing and Building National Research Center, Cairo, Egypt*
[c] *PhD Candidate, Cairo University, Egypt*

Received 10 August 2014; revised 28 October 2014; accepted 29 October 2014

KEYWORDS

Ultra high strength concrete;
Columns;
Cyclic load;
Steel fiber

Abstract In general Ultra High Strength Concrete (UHSC) is a new class of concrete that has been developed in recent decades. UHSC is characterized by extraordinary mechanical and durability properties. The UHSC-Matrix is very brittle material behavior. In this research an experimental program consists of twelve square UHSC columns is being carried out to study the behavior of UHSC columns subjected to constant axial load combined with cyclic lateral loading in order to simulate the case of seismic action. The main parameters of this program were: longitudinal reinforcement ratio, percentage of steel fiber, stirrups ratio, axial load level and concrete compressive strength. In this experimental program each specimen represents a column extending on both sides from the beam-column connection to the location of the point of inflection. Particular attention is paid to the effect of each variable on the strength enhancement, stiffness degradation, energy dissipation capacity, curvature ductility and displacement ductility of the tested columns. Valuable conclusions were obtained from the research results. By increasing the concrete compressive strength the column capacity increases accompanied by a decreasing in the ductility aspects, increasing the longitudinal steel ratio from 2% to (3.6% and 4.5%) leading to an increase in the column capacity and ductility aspect of the tested columns. Using steel fiber between (1.33–2.67)% is recommended in UHSC columns in seismic zones. The Egyptian concrete code of practice limits for the columns stirrups is suitable in seismic zones for columns subjected to a low axial load level.

* Corresponding author.
E-mail address: hoskarmoty@yahoo.com (H.Z. El-Karmoty).
Peer review under responsibility of Housing and Building National Research Center.

Production and hosting by Elsevier

Introduction

In the past several years an advance in the science of concrete materials have led to the improvement and development in the concrete technology. Sustainable use of supplementary materials and revolutionary developments in super plasticizing

http://dx.doi.org/10.1016/j.hbrcj.2014.10.003
1687-4048 © 2015 Production and hosting by Elsevier B.V. on behalf of Housing and Building National Research Center.

admixtures have facilitated in the mechanical properties and durability of concrete. For example researches are using silica fume and high range water reducing admixtures to produce high density concrete. In addition to high strength, the concrete should exhibit greater durability characteristics. This means that the concrete should be high strength and high performance. One of the materials developed in recent years is Ultra-High Strength Concrete (UHSC) also known as reactive powder concrete (RPC). This material possesses a compressive strength greater than 21,750 psi (150 MPa) [1].

In the case of reinforced concrete columns, it is necessary to allow for relatively large ductility without shear failure or significant strength degradation. It is well established that high ductility could be achieved in reinforced concrete members by furnishing a large amount of lateral confinement steel. When properly detailed, lateral steel would provide higher ductility, prevent premature buckling of main reinforcement, and avert shear failure [2]. It was investigated recently that the longitudinal steel has a small beneficial effect on the flexural ductility [3]. The amount of lateral steel required in structures where strength (and not ductility) is the primary design criterion is considerably less than that required in earthquake-prone areas. Using fibers for improving ductility and avoiding brittle behavior is a general way that has been widely investigated in the last few decades. Also it was found that the fiber plays a critical role in the ductile behavior of a structure until flexural failure [4] and it is addition in the H.S.C at any of the tested fiber contents did not increase the ultimate load of the column [5]. The axial load level has a beneficial influence on the moment resisting capacity and initial stiffness. However it also accelerates strength and stiffness degradation. The main objective of this research is to investigate the different parameters that affect the behavior of UHSC columns under axial and cyclic lateral loads.

Research significance

This paper presents the results of an experimental program which is being carried out to investigate the different parameters that affect the behavior of reinforced (UHSC) columns under axial and cyclic lateral loads, including steel fibers; the experimental program consists of twelve square UHSC columns. The main parameters were: longitudinal reinforcement ratio, percentage of steel fiber, axial load level, stirrups ratio and compressive strength. The test data are used to give proposed regulations for designing of UHSC columns located in seismic zones.

Table 2 Reference columns configurations [6].

Specimen	Main reinforcement	% ρ	F_{cu} (MPa)	% steel fiber	ρ_v	Axial load P
CR1	4Ø12	2	100	0	S = 7.5/15	0.2 P_0
CR2	4Ø12	2	50	0	S = 7.5/15	0.2 P_0
CR3	4Ø12	2	25	0	S = 7.5/15	0.2 P_0

Research program

The experimental program consists of twelve square UHSC columns have a total height of 2300 mm and a cross section of 150 × 150 mm. A clear cover of 15 mm thickness was provided to all specimens. Tables 1 and 2 show the configurations of experimental program of the tested specimens. The test variables include longitudinal reinforcement ratio, percentage of steel fiber, axial load level, stirrups ratio and compressive strength. The effect of the last parameter (compressive strength) was studied by using the results of three similar reference columns from a previous research [6] and were having a different compressive strength The beam stub, which was heavily reinforced, provided a point of application of lateral load and strengthening of the joint region so that any hinging will occur in the column rather than the joint and it locates at the midpoint of the column so that used instrumentation were at the two portions of column. Fig. 1 shows the concrete dimensions and steel reinforcement details of specimen C1.

Materials properties

The materials used in this study were coarse aggregate which was local crushed dolomite from natural resources with nominal maximum size of 5 mm, the fine aggregate was natural siliceous sand with grain size ranging from 0.15 to 0.5 mm, CEMI 42.5N of the Suez Company – Suez factory, Quartz powder used as a filler form with Blain fineness of 470 m^2/kg, and a specific gravity of 2.63, Clean drinking fresh water free from impurities, and chemical admixture. All concrete ingredients comply with the requirements of the Egyptian standard specifications. Silica fume was used as addition for the cement to produce workable concrete with high cubic compressive

Table 1 Columns configurations.

Specimen	Main reinforcement	% ρ	F_{cu} (MPa)	% steel fiber	ρ_v	Axial load P
C1	4Ø12	2	141	0	S = 7.5/15	0.2 P_0
C2	4Ø16	3.6	141	0	S = 7.5/15	0.2 P_0
C3	4Ø18	4.5	141	0	S = 7.5/15	0.2 P_0
C4	4Ø12	2	141	1.33	S = 7.5/15	0.2 P_0
C5	4Ø12	2	141	2.67	S = 7.5/15	0.2 P_0
C6	4Ø12	2	141	0	S = 10/20	0.2 P_0
C7	4Ø12	2	141	0	S = 5/10	0.2 P_0
C8	4Ø12	2	141	0	S = 7.5/15	0
C9	4Ø12	2	141	0	S = 7.5/15	0.35 P_0

The nominal column axial load capacity $P_0 = 0.67\ F_{cu}\ (A_g - A_{st}) + F_y * A_{st}$.
S: spacing of the transverse reinforcement.

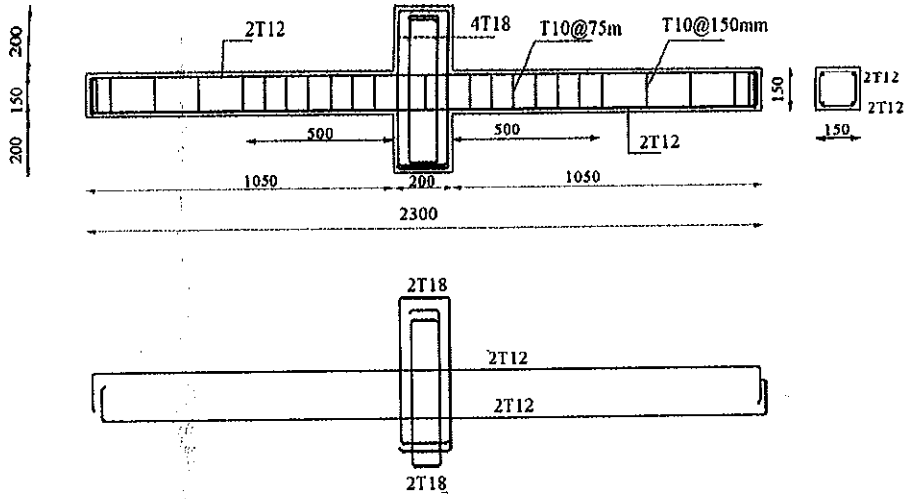

Fig. 1 Concrete dimensions and steel reinforcement details of specimen C1.

strength. Super-plasticizer was used to produce self-leveling concrete with only the water necessary for the hydration of the cement; the super-plasticizer used was high performance and was known as (Visocrete-20HE). Deformed high tensile steel of elastic strength of 420 MPa and ultimate strength of 630 MPa was used for all tested columns. Main reinforcement of 12, 16 and 18 mm diameter bars was used, while 10-mm diameter bars were used in stirrups. Steel fiber which has a bent bar shape with diameter 1.0 mm and average tensile strength 1298 MPa was used.

Fabrication of test columns

According to Khattab [7], the design cube compressive strength of the concrete was 141 MPa after 90 days. The concrete mix consists of 800 kg/m^3 cement content, 154 kg/m^3 water, 318.8 kg/m^3 quartz powder, 318.8 kg/m^3 siliceous sand, 637.5 kg/m^3 crushed dolomite, 160 kg/m^3 silica fume and finally 32 kg/m^3 super plasticizer. The fresh concrete had a 550 mm slump flow; it was closed to self-compacting concrete. Mixing is performed using a concrete drum mixer. Wooden forms were prepared for casting the concrete. Concrete was cast in under control laboratory conditions of 25 °C temperature. The specimens were moist cured after de-molding and have a stem curing for 2 days.

Test setup

Two independent reaction frames were used in the test program. The first frame is 2000 kN, large-scale testing double portal, open reaction frame, while the second frame is a 3000 kN closed horizontal reaction frame. The large frame consists of four A-frames, each of 4500 mm height and 3500 mm base length. The A-frames can be arranged and fixed on the laboratory rigid floor at any position according to the test requirement.

Four girders of depth 1000 mm and length 5300 mm were connected to the A-frames at different levels and positions (vertically or horizontally) according to the test requirements. To achieve the requirements of the test program, the A-frames and girders are arranged in the form of two opposite portal frames of spacing 3000 mm apart and connected to each other by using prestressed ties. The spacing between the legs of each portal frame is 3000 mm, and the bottom level of the girder is 3800 mm above the ground. A cross girder is mounted between the two portal frames to give a continuous line of support to the upward reactions. The bottom level of the cross girder is 2.80 m above the ground. The maximum vertical capacity of the frame according to this arrangement is 2000 kN.

The closed horizontal reaction frame consists of two square end plates of side length 1000 mm and thickness 200 mm which are tied together with four tie rods. The clear distance between the two plates varied from 2700 to 3500 mm according to the test needs. The clear space is taken 3350 mm in the test program. The clear space inside the frame in the lateral direction is 600 × 600 mm. The maximum capacity of the frame is 3000 kN. Two ball joints are mounted at the ends of the specimen to allow rotation at the ends of each specimen.

The closed horizontal frame is located under the cross girder of the double portal frame such that the centerline of the closed frame is oriented parallel to the line of support of the cross girder. The lateral reversed cyclic displacement is applied at the stub of the beam-column joint by using a double acting hydraulic cylinder of compression capacity 600 kN and tension capacity 400 kN. The hydraulic cylinder is attached to the cross girder of the double portal frame. The cylinder is equipped with tension/compression load cell of capacity ± 680 kN to measure lateral loads. The compression and tension lateral loads are transmitted to the specimen by two rigid plates located at the top and bottom of the stub and are tied together with four threaded ties around the stub. The higher plate is attached to the load cell. The axial compression load is applied by a manual hydraulic cylinder 2000 kN capacity. The two ends of the specimens were considered to be hinged and restrained only against vertical translations. The specimen is supported on two vertical concrete blocks 800 mm high and spaced 2100 mm apart. Each block is equipped with a hinged support at its top to permit rotations. The upward reaction is transmitted to the cross girder of the frame through two 500 kN hydraulic cylinders attached to the cross girder, each cylinder is equipped with threaded

Please cite this article in press as: M.M. El-Attar et al., The behavior of ultra-high-strength reinforced concrete columns under axial and cyclic lateral loads, HBRC Journal (2015), http://dx.doi.org/10.1016/j.hbrcj.2014.10.003

adjustment and an end ball bearing to permit rotation. At the beginning of the test, the ends of the specimens were well clamped against vertical translations by using the hydraulic cylinders. Fig. 2 illustrates the details of the test setup.

Instrumentation

Specimens were instrumented to obtain load displacement, moment curvature and reinforcement bars strain, as shown in Fig. 3. According to [8] a pairs of linear variable differential transducers (LVDTs) with stroke ± 20 cm and sensitivity 0.1 mm and another pairs of (Pi-gages) with length 10 cm and readability (± 10 mm) were mounted at the top and bottom sides of the right and left critical sections. There functions were to measure the concrete strain and the average section curvature over 200 mm length in the plastic hinge region. The lateral displacement control sensor used in testing is a long (LVDT) ± 10 cm stroke with 0.10 mm sensitivity. The sensor is mounted on a handling unit, which is located on the ground under the lateral load head. All the LVDTs and Pi-gages were attached to the specimen using 6 m fisher bolts. Three electrical strain gages were glued on the longitudinal reinforcement of each specimen. A load cell ± 680 kN capacity with 1 kN sensitivity was used to measure the applied lateral load throughout the test. The applied axial load was measured using a load cell ± 2000 kN capacity connected with a digital reader with 1 kN accuracy. The electrical strain gages and load cells voltages were fed into the data acquisition system. The voltage excitations were read, transformed and stored as micro strains, force and displacement by means of a computer program that runs under the Lab View software.

Test procedure

The specimens were subjected to a number of loading cycles while maintaining constant axial load. The axial load was applied first at a predetermined level during each test. The specimens were tested under quasi-static displacement control technique. At the beginning of each test, the specimen was centered in a horizontal position with the closed horizontal frame which allowed for minor adjustments and then anchored from the two ends by two hydraulic cylinder attached to the cross girder of the double portal frame. Vertical and horizontal loading systems were then positioned. The (LVDTs) and (Pi-gages) were adjusted in position. The strain gages, and electrical pressure sensors were hooked up to the data acquisition system and checked. To facilitate the detection of cracks in concrete, the surfaces of the specimens were white washed just

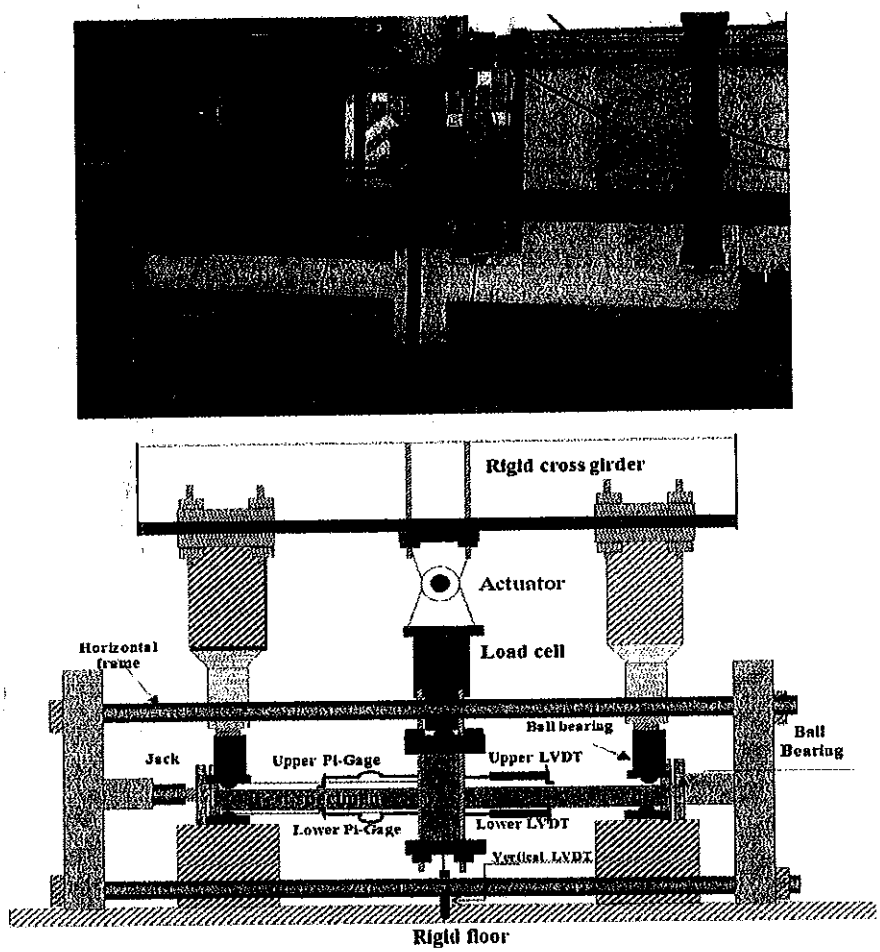

Fig. 2 Test setup.

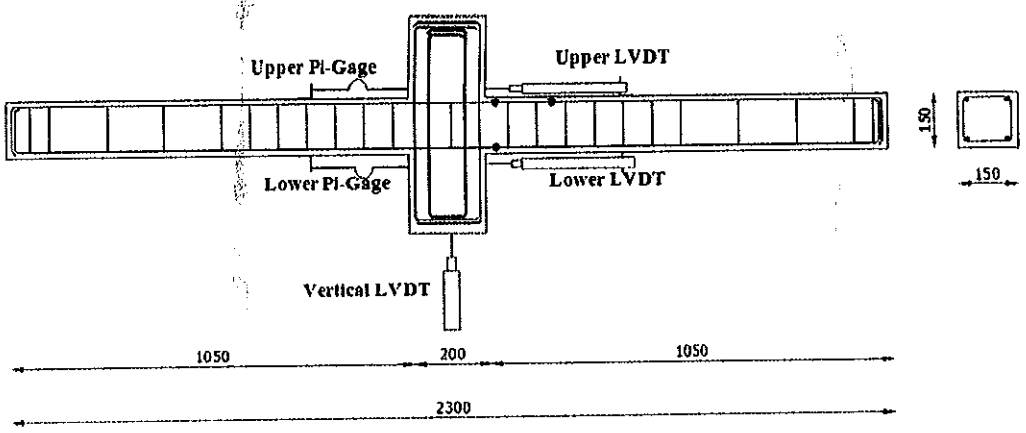

Fig. 3 Locations of horizontal LVDT, Pi-gages and strain gage in all test specimens.

before testing. The required axial load level was applied at the targeted value and kept constant throughout the test by re-adjusting the oil pressure in the manual hydraulic cylinder using its release valve. The testing program was activated and the electrical pump was switched on. The reversible hydraulic jack, which was controlled by automatic valve, started to apply an increasing cyclic lateral load in displacement increments. All of the data gathered from load cells, LVDTs, Pi gages and strain gages were continuously recorded during the test by the data acquisition system. Cracks were observed and marked for each load level. The test ended when one of the following events occurred:

- The column was not able to sustain the applied axial load which can be noticed by a sudden drop in the reading of the digital reader.
- Loading dropped to less than 75% of the maximum experienced capacity.

Test results

This section presents analysis of the test results to clarify the variation in cracking behavior, mode of failure, strength decay, stiffness degradation, ductility, curvature ductility and dissipated energy of the tested specimens. Moreover, measures are defined to quantify this variation of each specimen. Table 3 summarizes the outcomes of the experiments, the maximum load P_{max}, the cracking load P_{cr} and corresponding displacements (Δ_{cr} and Δ_u), also Table 4 summarizes the reference specimen outcomes. The ultimate moment level and number of failure cycles of each specimen are also included in the same table. Tables 5 and 6 show the values of the drift ratios, displacement ductility factors, curvature ductility factors and also energy dissipation indices for all tested and reference specimens.

In general, the displacement ductility factor is defined as the ratio between the displacement at failure load, Δf which is known as the displacement at 75% of the lateral load on the decreasing branch of the load–displacement envelope, and the yield displacement, Δy which is calculated from the lateral load–displacement curve as the corresponding displacement of the intersection of the secant stiffness at a load value of 75% of the ultimate lateral load and the tangent at the ultimate load [9]. The drift ratio is the ratio between the displacement at failure load and the specimen length (L), as shown in Eqs. (1) and (2) [10].

$$\text{Displacement ductility factor} = \Delta f/\Delta y \tag{1}$$

$$\text{Drift ratio} = \Delta f/L \tag{2}$$

The curvature ductility factor is the ratio between the failure curvature (Φf) which is known as the curvature at 75% of the ultimate moment on the decreasing branch of the moment–curvature envelope and the yield curvature (Φy) defined in a similar manner to Δy.

The energy index (Ie) which was proposed by Ehsani and Wight [11] as a reliable measure of the energy dissipation capacity is expressed as follows:

$$\text{Ie} = \left(\Delta E_i(K_i/K_y) * (\Delta i/\Delta_y)^2\right)/(P_y * \Delta_y) \tag{3}$$

where E_i is the dissipated energy at cycle number.

(K_i and K_y) are the stiffness at cycle number i and the stiffness at yield, respectively.

Δi is the average of maximum compression and tension displacements at cycle number i.

Δ_y, P_y are the yield displacement and yield load, respectively.

Discussion of test results

Evaluation of the major test variables on the behavior of the tested columns is discussed in the following subsections. Variables covered in this evaluation include the longitudinal reinforcement ratio, percentage of steel fiber, stirrups ratio, axial load level and compressive strength Particular attention is paid to the effect of each variable on the strength enhancement, stiffness degradation, energy dissipation capacity, curvature ductility and ductility of the tested columns.

Effect of longitudinal steel ratio (ρ)

Variation of longitudinal steel had a significant effect on the performance of the tested columns under cyclic loading. This effect can be presented by comparing the behavior of columns C1, C2, and C3 which had four 12-mm diameters, four 16-mm

Table 3 Values of cracking loads, ultimate loads, corresponding displacements, and number of failure cycles for all test specimens.

Specimen	Visible cracking level		P_{max} (kN)	Δ_{max} (mm)	M_{max} (kN)	P_{max}/P_{max} of C1	No. of failure cycle
	P_{cr}	Δ_{cr}					
C1	96.89	6.22	120.69	13.41	105	1	15
C2	73.97	5.07	131.6	17.21	114.49	1.09	18
C3	86.29	6.02	150.05	18.04	130.54	1.24	17
C4	76.8	4.2	134.32	12.17	116.83	1.11	16
C5	80.67	5.48	157.34	14.35	136.69	1.30	18
C6	68.59	5.27	119.8	16.17	104.36	0.99	17
C7	71.16	6.09	122.71	16.04	106.76	0.93	17
C8	31.48	5.07	63.35	24.37	55.12	0.53	21
C9	99.79	5.26	153.49	12.52	132.92	1.27	16

Table 4 Values of cracking loads, ultimate loads, corresponding displacements, and number of failure cycles for reference specimen [6].

Specimen	Visible cracking level		P_{max} (kN)	Δ_{max} (mm)	P_{max}/P_{max} of C1	Failure cycle
	P_{cr}	Δ_{cr}				
CR1	46.18	4.16	92.26	16.05	0.76	7
CR2	32.72	4.13	59.92	20.1	0.50	10
CR3	20.72	3.83	38.94	20	0.32	7

Table 5 Values of yield, failure displacements, drift ratios, displacement ductility factors, and energy indices for all test specimens.

Specimen	Yield displacement Δ_y (mm)	Failure displacement Δ_f (mm)	Drift ratio %	Displacement ductility factor	Curvature ductility factor $\emptyset_f/\emptyset_y$	Energy index
C1	10.2	16.2	1.54	1.60	1.5	222.3
C2	11.5	19.5	1.86	1.69	–	239.18
C3	11.8	19.8	1.89	1.68	1.86	231.55
C4	8.7	18.4	1.7	2.11	2.8	321.96
C5	10.9	20.9	1.99	1.93	2.44	292.8
C6	11	18	1.67	1.65	1.82	204.48
C7	10.9	18.4	1.68	1.72	2.0	286.39
C8	13	31.86	3.03	2.45	–	350.03
C9	9.2	14.7	1.40	1.56	3.9	184.24

Table 6 Values of yield, failure displacements, drift ratios, displacement ductility factors, and energy indices for reference specimen [6].

Specimen	Yield displacement Δ_y (mm)	Failure displacement Δ_f (mm)	Drift ratio %	Displacement ductility factor	Energy index
CR1	10.2	16.2	1.90	2.05	253.75
CR2	11.5	19.5	3.03	3	291.25
CR3	11.8	19.8	2.9	4.43	363.55

diameters, and four 18-mm diameters respectively. All these columns had the same compressive strength, stirrups ratio, axial load level, and steel fiber ratio. The hysteretic response of the three columns can be compared by examining the load–displacement envelopes, see Fig. 4. The ultimate loads of these columns were 100%, 109%, and 124% of that of column C1. Column C2 and C3 had an initial stiffness of 26.3% and 25.4% higher than that of C1. The displacement ductility factor increased only from 1.60 to 1.69, 1.68 for C1, C2, C3 respectively with increasing the longitudinal steel ratio from 2% to 3.6% and 4.5%. Also with the same trend the drift ratio increased from 1.54 to 1.86, 1.89 for C1, C2, C3 respectively, while the energy dissipation indices refers to a reduction in ductility with increasing the longitudinal steel ratio, where the energy dissipation index of C1, C2, and C3 were 222.3, 239.18 and 231.55 respectively which mean that the energy index for C2, C3 is more than C1 only by 7.6%, 4.16%. The curvature ductility factor is in the same trend as the displacement ductility factor such that it increased from 1.50 for C1 to 1.86 for C3 respectively with increasing the longitudinal steel ratio from 2% to 4.5%, but For C2 there is an reading error to determine this factor; see Figs. 5 and 6.

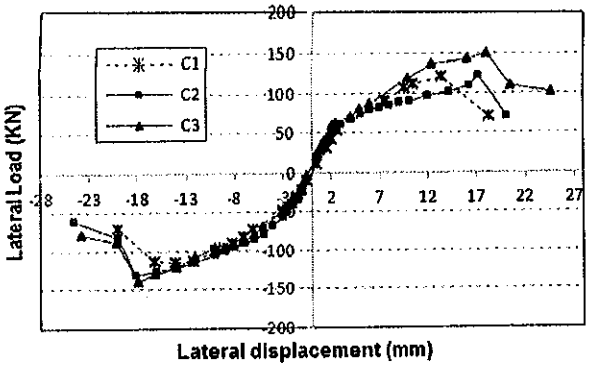

Fig. 4 Load displacement envelope for C1, C2, and C3.

It is obvious that changing the longitudinal steel ratio from 2% to (3.6% and 4.5%) effect the ductility aspects and the column capacity but there is no big change between the two ratios 3.6% and 4.5%. So, all the previous data indicated that the ratio of 3.6% longitudinal steel is suitable for UHSC columns subjected to seismic action from the ductility aspects point of view.

Effect of steel fiber ratio

Variation of steel fiber ratio had a significant effect on the performance of the test columns under cyclic loading especially from the ductility point of view. This effect can be presented by comparing the behavior of columns C1, C4, and C5 which had 0%, 1.33%, 2.67% of steel fiber respectively. All these columns had the same compressive strength, longitudinal steel, stirrups ratio and axial load level. The hysteretic response of the three columns can be compared by examining the load–displacement envelopes, see Fig. 7. The ultimate loads of these columns were 100%, 111%, and 130% of that of column C1 that means that increasing the steel fiber ratio increase the ultimate loads of the columns. The initial stiffness of the columns C1, C4, and C5 were 100%, 38.07%, and 18.9% respectively. The displacement ductility factor increased from 1.60 for C1 to 2.11 and 1.93 for C4, C5 respectively with increasing the steel fiber ratio from 0% to 1.33% and 2.67%. This increasing in the displacement ductility factor turns the column to have a satisfactory level of ductility. The drift ratio is almost gives the same indication of the displacement ductility factor, where

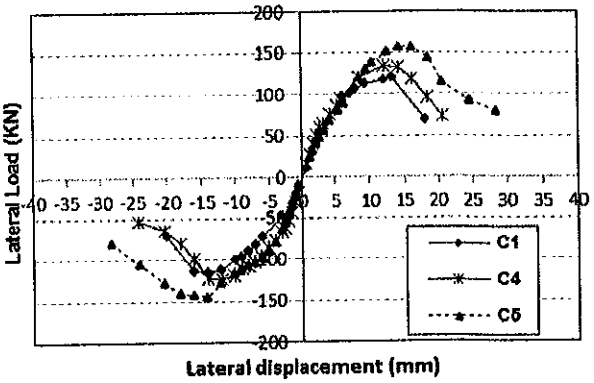

Fig. 7 Load displacement envelope for C1, C4, and C5.

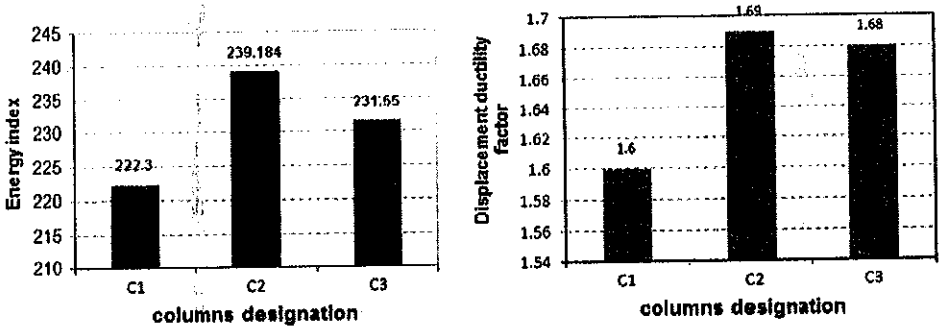

Fig. 5 Displacement ductility factor and energy index for C1, C2, and C3.

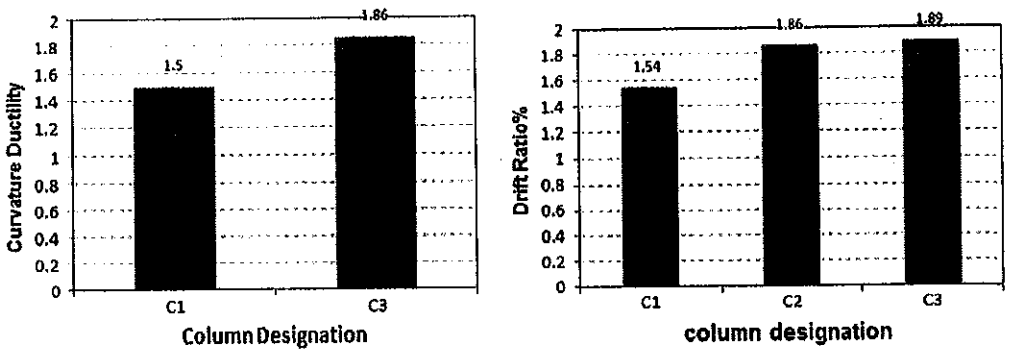

Fig. 6 Curvature ductility factor and drift ratio for C1, C2, and C3.

the drift ratio for C1 was 1.54% while for C4 and C5 were 1.7% and 1.9%. The energy dissipation index refers to the same increasing in ductility with increasing the steel fiber ratio only to 1.33%, where the energy dissipation index of C1, C4, and C5 were 222.3, 321.96, and 292.8 respectively. The curvature ductility factor is in the same trend as the displacement ductility factor such that it increased from 1.50 for C1 to 2.8 and 2.44 for C4, C5 respectively with increasing the steel fiber ratio from 0%, 1.33% to 2.67%; see Figs. 8 and 9.

The addition of high percentage of fibers resulted in a significant effect on the mode and mechanism of failure of this specimen. The fiber reinforced ultra high strength concrete failed in a more ductile mode. The addition of fibers transformed the brittle high strength cement composite into a more isotropic, ductile material and thus increase in the member ductility was observed. Failure mode of the tested specimens C1, C4, and C5 were shown in Fig. 10. It was observed that the ratio 1.33% improve the ductility aspects while the ratio 2.76 improve the columns capacity (ultimate Loads). So that all the previous data indicated that the suitable ratio of steel fiber for UHSC columns subjected to seismic action lies between (1.33–2.76%).

Effect of stirrups ratio

Variation of stirrups ratio had a significant effect on the performance of the test columns under cyclic loading especially from the ductility point of view. This effect can be presented by comparing the behavior of columns C7, C1 and C6 which had a stirrups spacing of 50 mm, 75 mm, and 100 mm respectively. All these columns had the same compressive strength, longitudinal steel, axial load level, and steel fiber ratio. The hysteretic response of the three columns can be compared by examining the load–displacement envelopes, see Fig. 11. The ultimate loads of C7, C1 and C6 were 101.7%, 100%, and 99.3% of that of column C1 respectively, that means increasing the stirrups spacing cause a reduction in the ultimate load and vice versa. The initial stiffness of the columns C1, C6, and C7 were 100%, 111.6% and 108.2% respectively. The displacement ductility factor varied from 1.60 for C1 to 1.65 and 1.72 for C6, C7 respectively with changing the stirrups spacing from 75 mm, 100 mm to 50 mm. For C6, C7 displacement ductility factor increased only by 3.13%, 6.25% compared to that of C1. The drift ratio increased in both C6 and C7 by 8.40% and 9.1% compared to that of C1. The curvature ductility for C1, C6 and C7 varied from 1.5, 1.82 and 2 respectively, see Figs. 12 and 13, so it was observed that the ultimate lateral load, the displacement ductility factor, drift ratio, energy index and the curvature ductility did not have a great difference in their values which means that changing the stirrups spacing from 75 mm (ρ_v = 3.6%) to 100 mm (ρ_v = 2.72%) or even to 50 mm (ρ_v = 5.4%) did not make a great effect on the behavior of UHSC columns under seismic action.

Consequently the Egyptian code for design and construction of concrete structures' limits for the columns stirrups ratio (3.6%) (spacing 75 mm) is suitable in seismic zones for columns subjected to a low axial load level. But, when the columns are subjected to a high axial load level, a significant

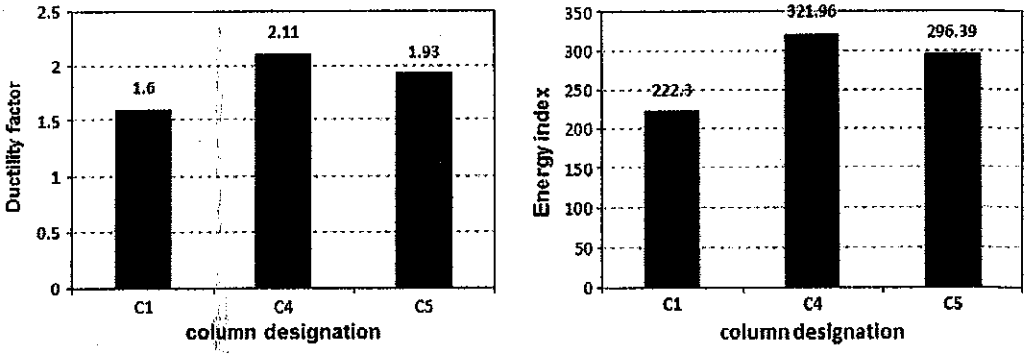

Fig. 8 Displacement ductility factor and energy index for C1, C4, and C5.

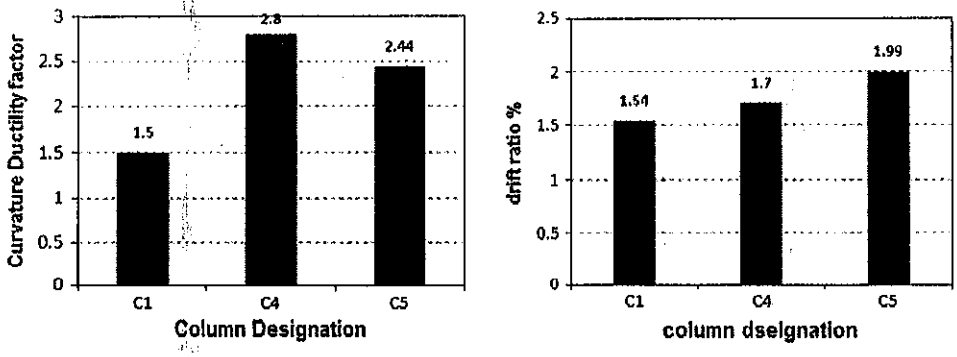

Fig. 9 Curvature ductility factor and drift ratio for C1, C4, and C5.

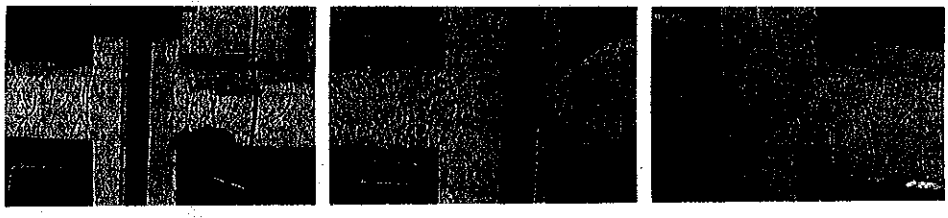

Fig. 10 Failure mode of specimens C1, C4, C5.

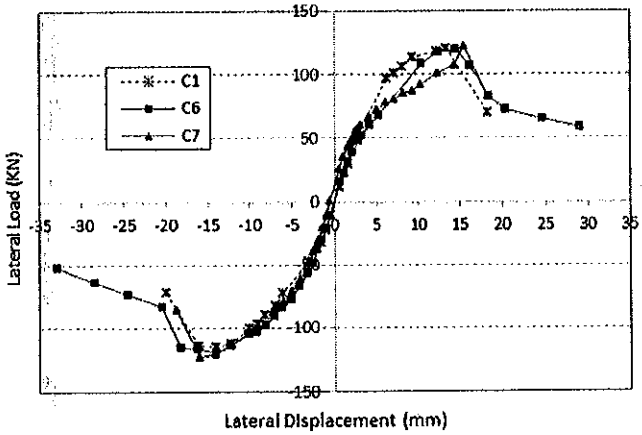

Fig. 11 Load displacement envelope for C1, C6, and C7.

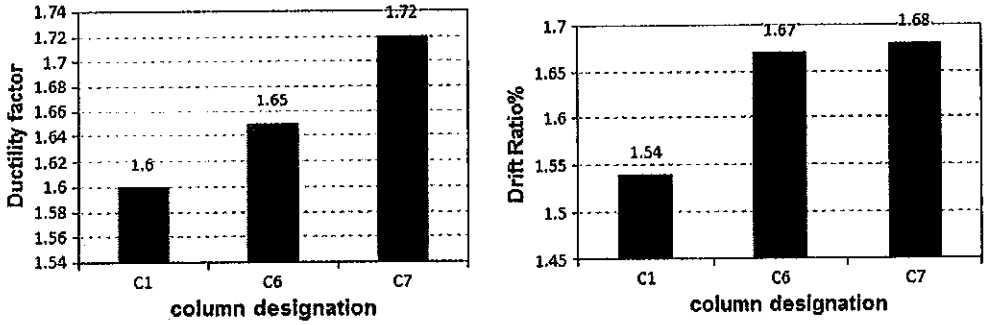

Fig. 12 Displacement ductility factor and drift ratio for C1, C6, and C7.

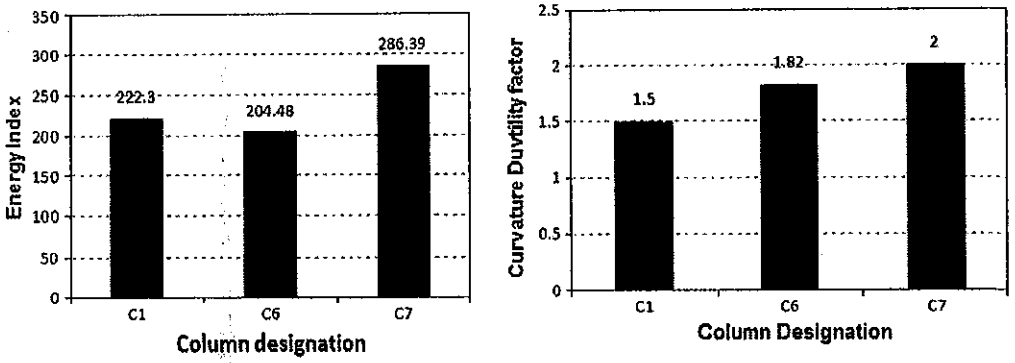

Fig. 13 Curvature ductility factor and energy index for C1, C6, and C7.

Please cite this article in press as: M.M. EL-Attar et al., The behavior of ultra-high-strength reinforced concrete columns under axial and cyclic lateral loads, HBRC Journal (2015), http://dx.doi.org/10.1016/j.hbrcj.2014.12.003

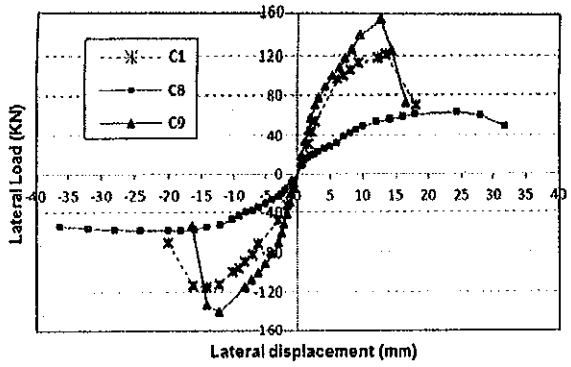

Fig. 14 Load displacement envelope for C1, C8, and C9.

amount of lateral steel is necessary. Ratios exceeding 3.6% must be use in practice. The safe, economical use of UHSC in seismic zones depends on relating the required ductility to the confinement detailing and amount of transverse reinforcement.

Effect of axial load level

Variation of axial load level had a significant effect on the performance of the test columns under cyclic loading. Three axial load levels were used, which were 0%, 20% and 35% of the nominal column axial load capacity P_0. This effect can be presented by comparing the behavior of columns C8, C1, C9 which had an axial load of zero, 630 kN (20% P_0) and 1110 kN (35% P_0) respectively. All these columns had the same compressive strength, longitudinal steel and stirrups ratio. The hysteretic response of the three columns can be compared by examining the load–displacement envelopes, see Fig. 14. The ultimate loads of C8, C1 and C9 were 52.5%, 100% and 127% respectively of that of column C1 that means increasing the axial load level has a great effect on increasing the ultimate load of the column under seismic action. The initial stiffness of the columns C8, C1 and C9 were 69.09%, 100% and 139.7% respectively. The displacement ductility factor varied from 1.60 for C1 to 2.45 and 1.56 for C8, C9 respectively. The drift ratio for C8, C1 and C9 were 3.03, 1.54 and 1.40 respectively. That means increasing level of axial load cause a significant reduction in ductility. The energy dissipation index refers to the same reduction in ductility with increasing the level of axial load, where the energy dissipation index of C8, C1, and C9 were 350.05, 222.3, and 184.24 respectively; see Figs. 15 and 16. The curvature ductility's for C1 and C9 were 1.5 and 3.90 respectively.

All the previous data indicated that the axial load level has a beneficial influence on the ultimate load and stiffness but it has a negative effect on the seismic behavior of the UHSC columns and it also accelerates strength and stiffness degradation. So, when the columns are subjected to a high axial load level, a significant amount of lateral steel is necessary.

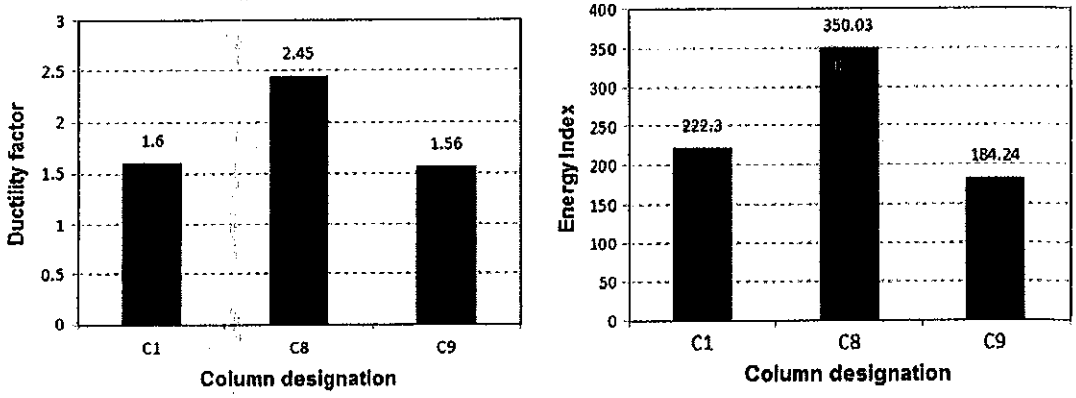

Fig. 15 Displacement ductility factor and energy index for C1, C8, and C9.

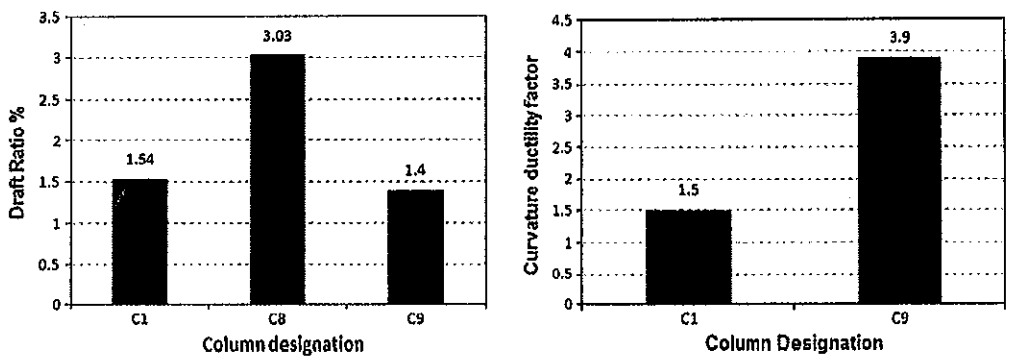

Fig. 16 Curvature ductility factor and drift ratio for C1, C8, and C9.

Where using 1.33% and 2.67% steel fiber enhance the displacement ductility factor by 31.9% and 20.6% respectively and the energy index by 44.8% and 31.7%. Also the same percentage improved the initial stiffness by 38.07% and 18.9% compared to the control specimen which had no steel fiber, it is obvious that the using 1.33% steel fiber has a greatest effect on the ductility aspects but using 2.67% steel fiber is more effective on the ultimate lateral load. So it can be concluded that the suitable steel fiber ratio which is recommended in UHSC columns in seismic zones lies between (1.33% and 2.67%)

3. The concrete compressive strength beneficial influence were shown when comparing the columns (C1, CR1, CR2 and CR3) with compressive strengths 150, 100, 50 and 25 MPa respectively as their ultimate loads were about 100%, 76.4%, 49.6% and 32.3% respectively of that of column C1 that means that increasing in the compressive strength has a valuable effect on increasing the ultimate load of the column under seismic action. In the same manner the stiffness values were less than the control specimen C1 by 36.43%, 47.56%, and 65.90%. In contrast increasing the compressive strength causes a significant reduction in ductility factor, drift ratio and energy index, so that the compressive strength has a negative effect on the seismic behavior of the UHSC columns and it also accelerates strength and stiffness degradation.
4. The axial load level has a beneficial influence on the ultimate load and stiffness, by increasing the axial load from zero to (20% P_0) to (35% P_0), the ultimate load increase from 63.35 to 120.69 to 153.49 kN but it has a negative effect on the seismic behavior of the UHSC columns such that a significant reduction in ductility factor, drift ratio and energy index, appear by increasing the axial load level and it also accelerates strength and stiffness degradation. So, when the columns are subjected to a high axial load level, a significant amount of lateral steel is necessary. Ratios exceeding
5. The Egyptian code for design and construction of concrete structures' limits for the columns stirrups ratio is suitable in seismic zones for columns subjected to a low axial load level. But, when the columns are subjected to a high axial load level, a significant amount of lateral steel is necessary. Ratios exceeding 3.6% must be use in practice.

References

[1] Allena S, Newtson M, Ultra-high strength concrete mixtures using local materials. In: Concrete sustain conference; 2010.
[2] N. Wehbe, M. Saiid, D. Sanders, Seismic performance of rectangular bridge columns with moderate confinement, J ACI Struct (1999).
[3] A. Kwan, J. Lam, Effectiveness of adding confinement for ductility improvement of high-strength concrete columns, J Eng Struct 32 (2010) 714–725.
[4] S. Kang, Y. Lee, Y. Park, J. Kim, Tensile fracture properties of an ultra high performance fiber reinforced concrete with steel fiber, J Compos Struct (2009).
[5] M.N.S. Hadi, Using fibers to enhance the properties of concrete columns, J Constr Build Mater (2005).
[6] A. Belal, Z. El-Karmoty, A. Abdelrahman, A. El-Dieb, H. Bahnasawy, S. Okba, The behavior of high strength reinforced concrete columns under axial and cyclic lateral loads, J HBRC 6 (2010) 71–79.
[7] Khattab E. Production of ultra high strength concrete using local materials and its application in axially loaded columns. Ph.D thesis. Ain Shams University; 2010.
[8] Elrakib T. Behavior of concrete columns retrofitted by fiber reinforced polymers under axial and cyclic loads. Ph.D thesis. Benha University; 2005.
[9] R. Park, Evaluation of ductility of structures and structural assemblages from laboratory testing, Bull NZ National Soc Earthquakes Eng 22 (1989) 155–165.
[10] P. Paultre, F. Légeron, Behavior of high-strength concrete columns under cyclic flexure and constant axial load, ACI Struct 97 (2000) 591–601.
[11] M. Ehsani, J. Wight, Confinement steel requirement for connections in ductile frames, J ASCE Struct 116 (1990) 751–767.

Please cite this article in press as: M.M. EL-Attar et al., The behavior of ultra-high-strength reinforced concrete columns under axial and cyclic lateral loads, HBRC Journal (2015), http://dx.doi.org/10.1016/j.hbrcj.2014.10.003